In: 2024 International Radar Conference (RADAR), 21-25 October 2024, Rennes, France
DOI:10.1109/radar58436.2024.10993546

CFAR Detection in Heterogeneous K-Distributed Sea-Clutter Background

Nagarakshith Mungara[1], Alessio Balleri[1], Leon Kocjancic[2] and Tim Acland[2]
[1]Centre for Electronic Warfare, Information and Cyber, Cranfield University,
Defence Academy of the United Kingdom, Shrivenham, SN6 8LA
[2]Hensoldt UK, Enfield, England, United Kingdom, EN3 7XQ
Rakshith.mungara@cranfield.ac.uk

***Abstract*—Detection of targets at sea is challenging due to unwanted echo returns from the sea surface, i.e. sea clutter returns. To account for the undesired effects of sea clutter at the receiver, and to control the probability of detection and false alarm, the K-distribution has often been used to provide a promising statistical fit to real clutter data. However, controlling the performance of the receiver becomes very challenging in heterogeneous clutter, that is when there is a sudden transition from one clutter region to another with a change in shape and/or scale distribution parameters. A possible solution to this challenge is to use some prior information on the sea clutter characteristics to generate clutter maps that inform adaptive detection solutions. This prior information can be obtained by the radar in real time (or close to real time) using oceanographic models, statistical clustering or potentially Artificial Intelligence.**

This paper presents our first step in this direction by investigating detection in heterogeneous fully correlated K-distributed sea clutter. A transition line between homogeneous clutter regions is estimated using the statistical parameters of a K-distribution, to avoid polluting the training windows of a Constant False Alarm Rate (CFAR) detector with non-representative data. The transition cells assist to resolve the heterogeneous clutter into small homogeneous clutter regions and for every homogeneous region a CFAR detector is designed according to the K-distribution shape parameter. Results are obtained and presented for simulated data as well as for real sea clutter data provided by Hensoldt UK.

***Index Terms*—Sea clutter, K-distribution, CFAR, Probability of False alarm, Probability of Detection**

I. Introduction

Unpredictable changes on the sea surface challenge statistical models which are used to characterise sea clutter and to estimate sea clutter parameters. Because of this, performance of the radar reduces in both detection capability as well in maintaining controlled and constant false alarm rates. Modern radars have high-resolution capability and can resolve small patches of the sea surface. As a result, data collected by modern radar does not meet the assumptions required for recalling the central limit theorem and clutter can no longer be modelled with a classic Gaussian distribution.

Previous research on clutter has focused on accelerating the development of non-Gaussian distributions to model sea clutter returns. Researchers have, for example, proposed the Log-Normal, Weibull, K and many other non-Gaussian distributions to characterise sea radar returns [1]–[3]. Sea clutter returns were characterised in [4] with the Log-Normal and contaminated Normal statistical models. Sea clutter was modelled by using the Weibull distribution, and radar detection performance using the Rayleigh, Log-Normal and Weibull distributions was compared in [5]. Long tailed, spiky sea clutter returns were modelled by a K-distribution in [6]. Later, K-distributed clutter was formulated as a compound clutter model consisting of the product of two independent components called texture and speckle [7]. The texture models the slow signal variations generated by swells and the speckle models the fast variation signals which are generated by ripples on the swells. In addition to these models, there have been some other models proposed to fit sea clutter such as compound Gaussian [8], compound Gaussian with Log-Normal texture [9], [10] and Inverse Gamma texture [11]. An adaptive target detection solution was proposed in compound Gaussian sea clutter with Inverse Gamma texture in [12].

Constant False Alarm Rate (CFAR) detectors maintain the false alarm rate constant in the presence of fluctuating interference, by estimating the interference level and adjusting the detection threshold. An Adaptive Censoring Maximum Likelihood Constant False Alarm Rate Detector (ACML-CFAR) for spiky Weibull clutter was proposed in [13]. Analysis of CA-CFAR performance was carried out in homogeneous Weibull clutter for shape parameters greater or equal to 1 in [14]. A constant false alarm rate detector based on the clutter data Skewness (SK) and Mean Ratio (MR), named SKMR-CFAR, was proposed for non-homogeneous Weibull clutter and multiple targets in [15]. Cell averaging CFAR was designed in an unknown Gamma distributed clutter background in [16]. A CFAR algorithm was designed for fully correlated texture in K-distributed sea clutter in [17].

Radar detection performance reduces when there is heterogeneous clutter. A modified Generalised K-distribution was proposed to mitigate detection capability losses with the K-distribution in heterogeneous environments in [18]. Another way to enhance detection capability in heterogeneous clutter data is to divide the data into a subset of homogeneous regions. Using this solution, a CFAR algorithm was developed for Rayleigh and Log-Normal clutter in [19]. In addition, CFAR performance was analysed in heterogeneous Weibull Sea clutter in [20]. By using a windowing method, heterogeneous data was separated into homogeneous data sections in [21].

Oceanography models that exist can potentially provide useful information on the sea parameters and the modelling

Published by IEEE. This is the Author Accepted Manuscript issued with: Creative Commons Attribution License (CC:BY 4.0).
The final published version (version of record) is available online at DOI:10.1109/radar58436.2024.10993546. Please refer to any applicable publisher terms of use.

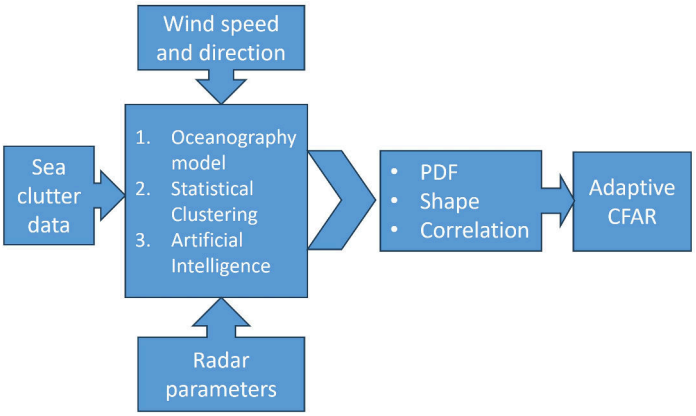

Fig. 1. Methodology for designing adaptive CFAR using prioir information.

of sea clutter, using the data collected by the radar itself in real time or close to real time [22], [23]. These models can be potentially used to create clutter maps and exploited to provide prior information of the clutter parameters, such as correlation properties, clutter power, type of distribution etc. Other methods that can provide this prior information include Statistical Clustering (e.g. [19] and [17]) and Artificial Intelligence (AI). By using prior information, adaptive CFAR solutions can be designed based on a detection strategy as shown in Fig. 1, where prior information is used to adapt the detection threshold according to a clutter region of interest.

In this paper, an initial step has been taken to address the idea of designing a detection algorithm by using oceanographic models to characterise the sea clutter. The algorithm described in [17] and [19] are used to provide a CFAR solution for fully correlated K-distributed clutter with different shape and scale parameters from region to region. Initially, the clutter maps are built by dividing the heterogeneous regions into homogeneous regions by maximising a log-likelihood function, from which a transition point is estimated [19]. Then a Cell Averaging Constant False Alarm Rate algorithm (CA-CFAR) is applied separately on both regions. This algorithm is tested on both simulated and real sea clutter data collected with the Mk11 ShapeEye X-band radar produced by Hensoldt UK [24]. The results show that the clustering algorithm efficiently identifies the regions with different clutter parameters and CFAR detection on real data. These heterogeneous algorithms were not explored on K-distributed clutter in the past.

II. Clutter Model

We consider a square law detector which models the amplitude square of the sea clutter return Z as the product of two terms

$$Z = TS \tag{1}$$

where, $T \sim \Gamma(\alpha, \beta)$ represents a texture component that follows a Gamma distribution with shape parameter α and scale parameter β and $S \sim \exp(1)$ represents a speckle component that follows an exponential distribution with mean value equal to one. Under these assumptions

$$p_T(t) = \frac{\beta^\alpha}{\Gamma(\alpha)} t^{\alpha-1} e^{-\beta t} \tag{2}$$

and

$$p_S(s) = e^{-s} \tag{3}$$

The probability density function of Z is found by using the Bayes theorem

$$\begin{aligned} p_Z(z) &= \int_0^\infty \frac{1}{t} p_S\left(\frac{z}{t}\right) p_T(t)\, dt \\ &= \frac{2}{\Gamma(\alpha)} \beta^{\frac{\alpha+1}{2}} z^{\frac{\alpha-1}{2}} K_{\alpha-1}(2\sqrt{\beta z}) \end{aligned} \tag{4}$$

and leads to a K-distribution.

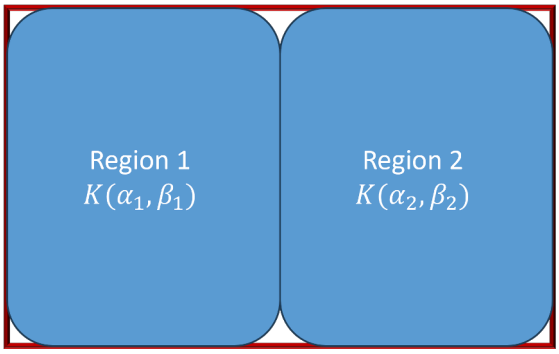

Fig. 2. Clutter region transition.

III. Estimate the Transition Cell

Two clutter regions are considered as shown in Fig. 2. In each region, the clutter follows a K-distribution but is described by different shape and scale parameters to represent an heterogeneous clutter scene. In this paper, we are mostly concerned with changes in shape parameter because the employed CFAR detector (see Eq.14) is independent of the scale parameter and does not affect false alarm rates. It is assumed the clutter is K-distributed and fully correlated so that the speckle is considered independent and the texture constant within a processing data window.

The estimators of the shape and scale parameters of a K-distribution can be found in [25] and expressed as

$$\begin{aligned} \frac{1}{\hat{\alpha}} &= \frac{\langle \mathbf{Z} \log \mathbf{Z} \rangle}{\langle \mathbf{Z} \rangle} - \langle \log \mathbf{Z} \rangle - \frac{1}{L} \\ \hat{\beta} &= \frac{\hat{\alpha}}{\langle \mathbf{Z} \rangle} \end{aligned} \tag{5}$$

where, the operator $\langle \mathbf{W} \rangle = \frac{1}{L} \sum_{l=1}^{L} W_l$ indicates the mean value of the L-element data vector $\mathbf{W}$. The vector $\mathbf{Z}$ represents the L-element window of homogenous clutter data used to estimate the shape and scale parameters.

When $\mathbf{Z}$ is a vector of heterogenous data, consisting of two

homogenous clutter regions, the Log-likelihood function of the index representing the transition cell M $(M < L)$ is

$$\log(L_M(m)) = \log\left(\prod_{i=1}^{m}(K(Z_i;\hat{\alpha_{1m}},\hat{\beta_{1m}}))\right)\times \log\left(\prod_{k=m+1}^{L}(K(Z_k\hat{\alpha_{2m}},\hat{\beta_{2m}}))\right) \quad (6)$$

where $(\hat{\alpha}_{1m},\hat{\beta}_{1m})$ and $(\hat{\alpha}_{2m},\hat{\beta}_{2m})$ are the estimates of the shape and scale parameters obtained from the vectors $\mathbf{Z}_{1m} = [Z_1 \,..\, Z_m]$ and $\mathbf{Z}_{2m} = [Z_{m+1} \,..\, Z_L]$ for m between 1 and $L-1$. There will be a value of m where $\log(P_M(m))$ is maximised. By maximising the log-likelihood function, the transition cell M can be estimated as

$$M = argmax\log(L_M(m)) \quad (7)$$

Once M is estimated, the final K-parameters are estimated from their respective clutter regions. The maximum log-likelihood algorithm to estimate the transition cell in (6) assumes $\mathbf{Z}_{1m}$ and $\mathbf{Z}_{2m}$ are statistically independent.

IV. Design of CA-CFAR

Sea clutter is modelled as K-distributed with fully correlated Gamma texture and independent exponentially distributed speckle. In the single sided Cell-Averaging CFAR (CA-CFAR) algorithm, the power is estimated with N reference samples adjacent to the Cell Under Test (CUT). The mean clutter power $\hat{\gamma}$ is estimated as

$$\hat{\gamma} = \frac{1}{N}\sum_{i=1}^{N} Z_i = \frac{1}{N}\sum_{i=1}^{N} TS_i = TX \quad (8)$$

and the threshold $\nu = \hat{\gamma}\tau$ is derived from the product of the estimated mean clutter power and a CFAR constant. A target is declared when the CUT is above the threshold [26].

Because of the assumption of a fully correlated texture, the Probability Distribution Functions (PDF) of $p(\hat{\gamma})$ is

$$p(\hat{\gamma}) = \int_0^\infty \frac{1}{t} p_X\left(\frac{\hat{\gamma}}{t}\right) p_T(t)\, dt \quad (9)$$

where $p_X\left(\frac{\hat{\gamma}}{t}\right)$ is the PDF of the mean of independent exponential random variables with equal mean value X, and $p_T(t)$ is the Gamma distribution. By using the PDF of the sum of exponential random variables from [27], the PDF of $p(\hat{\gamma})$ becomes

$$p(\hat{\gamma}) = \frac{2}{\Gamma(N)\Gamma(\alpha)}\beta^{\frac{\alpha+N}{2}}\hat{\gamma}^{\frac{\alpha+N}{2}-1}K_{\alpha-N}(2\sqrt{\beta\hat{\gamma}}) \quad (10)$$

A. Probability of false alarm

To determine the probability of false alarm $P_{fa} = P(Z > \nu)$, the Bayes Theorem is recalled and the conditioned probability is used with respect to the mean clutter power estimator $\hat{\gamma}$ as

$$P_{fa} = \int_0^\infty P(Z > \nu|\hat{\gamma})\, p(\hat{\gamma})\, d\hat{\gamma} \quad (11)$$

where, $P(Z > \nu|\hat{\gamma})$ can be calculated by integrating (4) from the threshold to infinity as

$$P(Z > \nu|\hat{\gamma}) = \int_{\hat{\gamma}\tau}^\infty \frac{2}{\Gamma(\alpha)}\beta^{\frac{\alpha+1}{2}} z^{\frac{\alpha-1}{2}} K_{\alpha-1}(2\sqrt{\beta z})\, dz \quad (12)$$
$$= \frac{2}{\Gamma(\alpha)}\beta^{\frac{\alpha}{2}}(\hat{\gamma}\tau)^{\frac{\alpha}{2}}K_\alpha(2\sqrt{\beta(\hat{\gamma}\tau)})$$

By substituting (10) and (12) in (11), the probability of false alarm can be written as

$$P_{fa} = \frac{4}{\Gamma(N)\Gamma(\alpha)^2}\beta^{\frac{2\alpha+N}{2}}(\tau)^{\frac{\alpha}{2}}\times \int_0^\infty (\hat{\gamma})^{\alpha+\frac{N}{2}-1}K_{\alpha-N}(2\sqrt{\beta\hat{\gamma}})K_\alpha(2\sqrt{\beta(\hat{\gamma}\tau)})\, d\hat{\gamma} \quad (13)$$

The integral can also be expressed in closed form by using the Hypergeometric special function ${}_2F_1$ from [28] as

$$P_{fa} = \left(\frac{\tau}{N}\right)^\alpha \frac{\Gamma(2\alpha)\Gamma(\alpha+N)}{\Gamma(\alpha)\Gamma(2\alpha+N)} \times {}_2F_1\left(2\alpha, \alpha+N, 2\alpha+N, 1-\frac{\alpha}{N}\right) \quad (14)$$

This equation is known in the existing literature [17] and shows that the scale parameter does not affect the false alarm performance because P_{fa} is independent of the scale parameter.

V. Results

The algorithms were initially tested on simulated heterogeneous K-distributed sea clutter data. To begin with, two regions of fully-correlated K-distributed clutter data were generated with parameters $K(\alpha_1 = 5, \beta_1 = 2.5)$ and $K(\alpha_2 = 10, \beta_2 = 5)$, respectively. This step provided a sea clutter data matrix consisting of 10^4 rows and 10^4 columns, for a total of 10^8 samples, with equal clutter regions made of 10^4 rows and 5000 columns. In the simulations, each row identifies an aspect angle and each column identifies a range bin. The transition line between the two regions was a straight line across the rows (i.e. at a constant range) and the transition cell was estimated along the range bins for each look aspect angle, with an expected transition cell at the 5001^{th} column. Fig. 3 shows a single row of the simulated data vector with the estimated transition cell location. The red points in Fig. 4 show the results of the estimated transition line between the two regions over the entire data matrix. Once the regions were resolved the shape and scale parameters were estimated in their respective regions. It should be noticed, that the estimation algorithm for the transition cell works also when

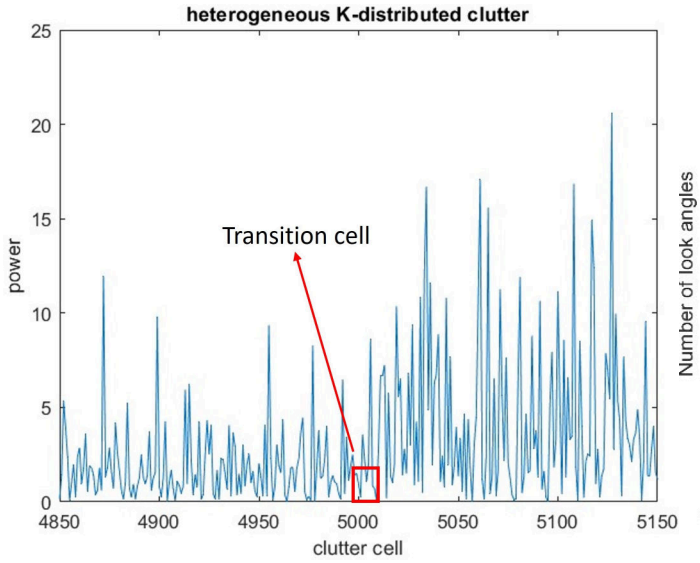

Fig. 3. Estimation of transition cell

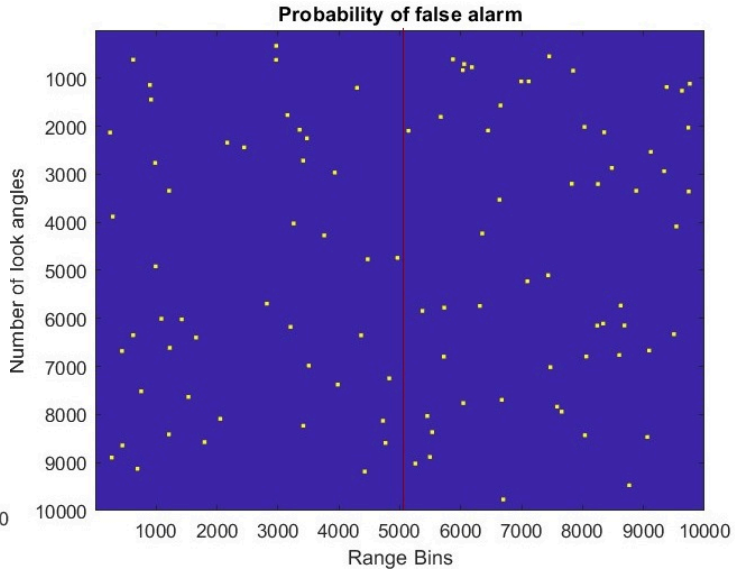

Fig. 5. CFAR algorithm tested on simulated heterogeneous data for desired $P_{fa} = 10^{-6}$

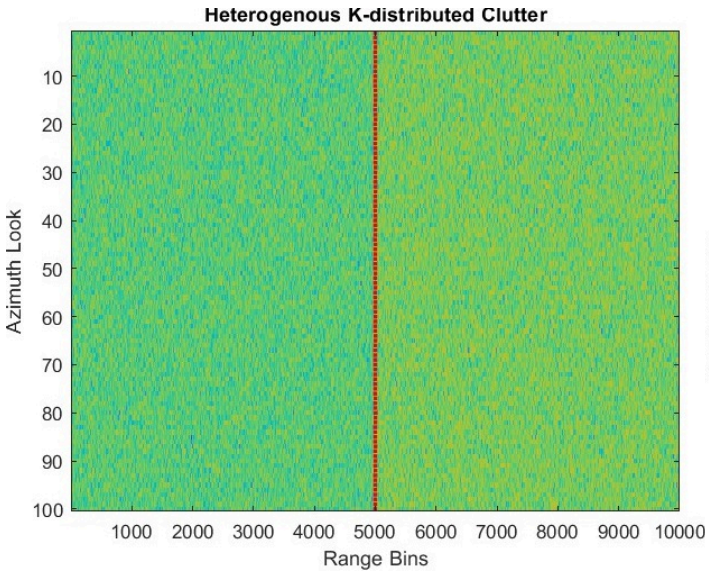

Fig. 4. Estimation of transition cells

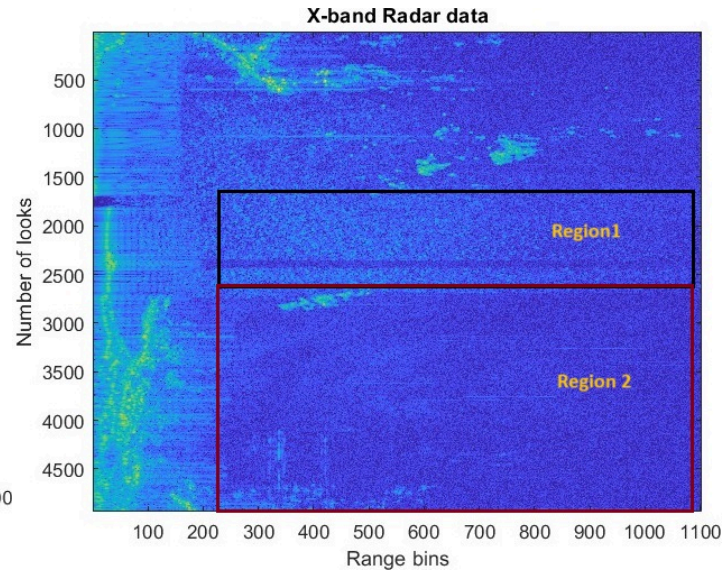

Fig. 6. Real X-band Radar data

the size of the regions is unequal. However, because the data follows a fully correlated K-distribution, and the maximum log-likelihood function of the parameters assumes independent K-distributed data, errors in estimating the transition cell can be expected. The fully correlated K clutter CA-CFAR detector [17], for a desired $P_{fa} = 10^{-6}$ with $N = 16$ reference windows, was applied (single sided) to the simulated data to analyse CFAR performance. Fig. 5 shows the results of the CFAR simulation. Result shows that the false alarms due to the clutter edge are suppressed and the desired P_{fa} is obtained despite the heterogeneous environment. Using the information on the estimated transition cell, the relevant estimated CFAR parameters could be used in each regions. This prevented from polluting the training windows with data from the two different statistical distributions.

Real sea clutter data was collected with the Mk11 X-band Radar by Hensoldt UK. The radar operates at 9.22 GHz with a Pulse Repetition Frequency (PRF) of 1.647 kHz, and transmits 8 μs long pulses to a maximum range of 24 Nm. The Mk11 SharpEye X-band Radar is a mechanical scanning radar with an update interval of 3 seconds. The antenna beam has a width equal to 0.9° in azimuth and rotates with a speed of 20 Rotations Per Minute (RPM). The radar has a range resolution of 15 m, uses 16 Doppler channels and achieves a Doppler resolution of 3 m/s. Fig. 6 shows the real data collected by the radar. A visual inspection of the data indicates the clutter is not homogenous with the presence of different clutter regions,

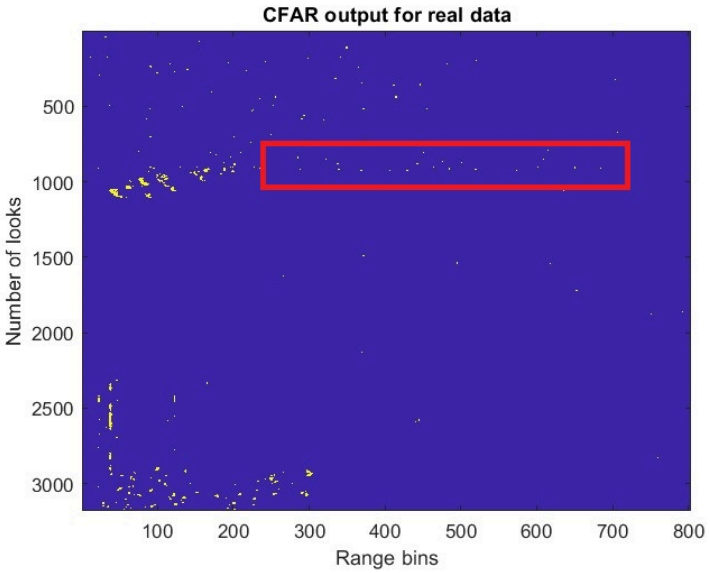

Fig. 7. CFAR algorithm tested on complete region

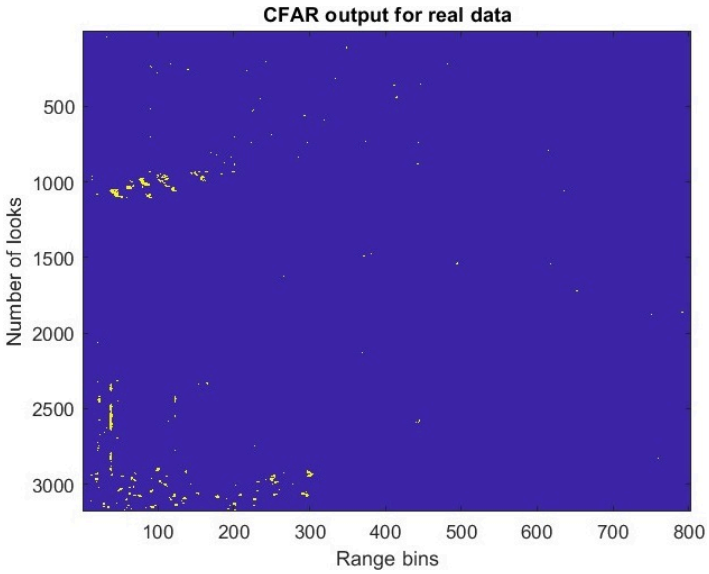

Fig. 9. Final Detection output from CFAR

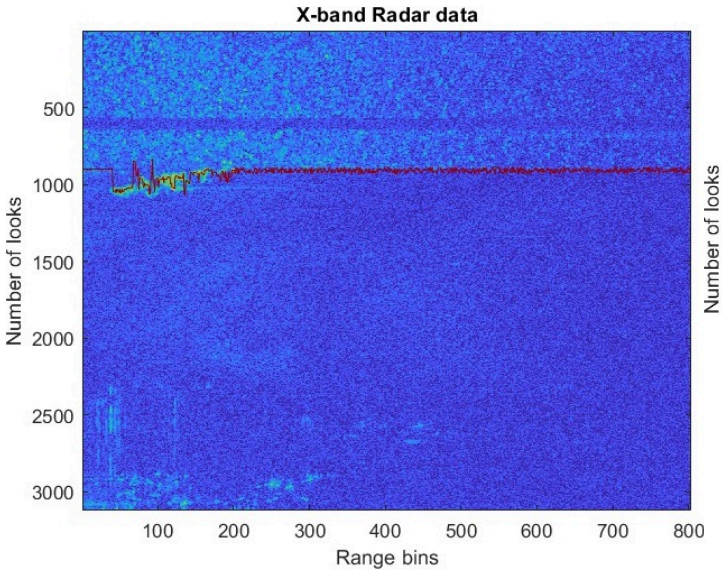

Fig. 8. Estimation of transition cells.

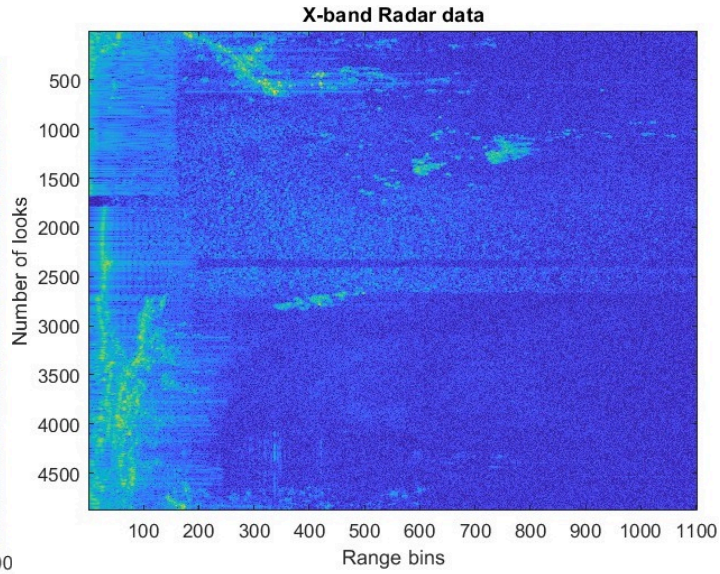

Fig. 10. Real X-band Radar data for 2^{nd} scan

two of which have been marked in the figure.

The same CA-CFAR algorithm used for the simulated data, set to achieve a $P_{fa} = 10^{-3}$ with $N = 16$ reference windows, was firstly applied to the entire experimental data with no attempts to separate the clutter into homogenous regions. The results relative to this case are shown in Fig. 7 and show a high false alarm rate along the clutter edges visually identified in Fig. 6. In this case, a false alarm of 0.0033 was obtained. To estimate the transition cells between homogenous regions, the algorithm proposed in this paper was then applied to the data along the range bins and along different look aspect angles. Fig. 8 shows the transition line between the regions in real data. Fig. 9 shows the CFAR results for this case where the false alarm rate of 0.0016 was achieved. Fig. 10 and Fig. 11 show the same results for a different radar scan to corroborate the results are consistent for different scans. In this case, the false alarm rate of 0.00155 was obtained. Overall, results also show that although the CFAR was designed to obtain a $P_{fa} = 10^{-3}$, higher experimental rates were obtained. This is likely due to the assumptions made on the experimental clutter statistics and correlation properties not being fully met by the real data.

VI. CONCLUSION

This work reports an algorithm to reduce false alarms along the clutter edge in heterogeneous fully correlated K-distributed clutter. A transition line is estimated between homogeneous

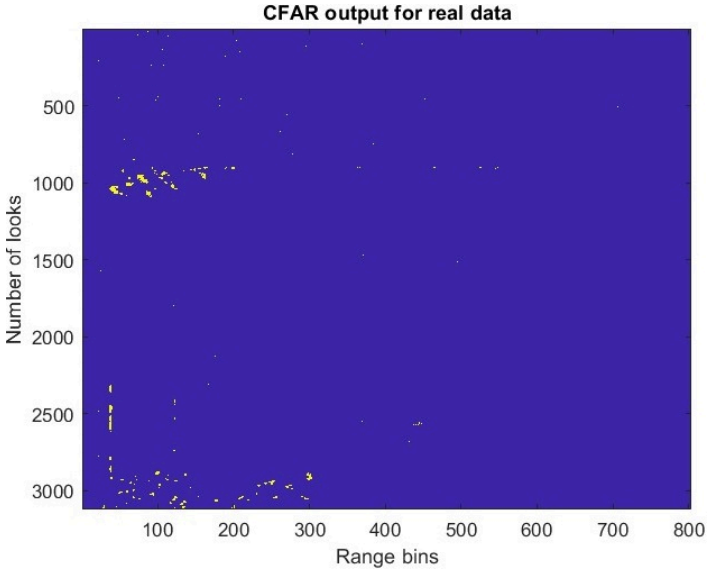

Fig. 11. Final Detection output from CFAR for $2^{n.d}$ scan

clutter regions and the shape and scale parameters are estimated from the respective homogeneous clutter regions. A single sided CA-CFAR algorithm was applied to individual homogeneous regions. Results showed the algorithm suppresses the false alarms due to clutter edges. Findings are applied to the real sea clutter data collected by a X-band maritime RADAR.

ACKNOWLEDGMENT

The authors thank Hensoldt UK and Cranfield University for jointly funding this PhD programme under the Cranfield Industrial Partnership PhD Scholarships Scheme (CIPPS)

REFERENCES

[1] K. Sangston and K. Gerlach, "Coherent detection of radar targets in a non-gaussian background," *IEEE Transactions on Aerospace and Electronic Systems*, vol. 30, no. 2, pp. 330–340, 1994.

[2] E. Conte and G. Ricci, "Sensitivity study of glrt detection in compound-gaussian clutter," *IEEE Transactions on Aerospace and Electronic Systems*, vol. 34, no. 1, pp. 308–316, 1998.

[3] N. Pulsone and R. Raghavan, "Analysis of an adaptive cfar detector in non-gaussian interference," *IEEE Transactions on Aerospace and Electronic Systems*, vol. 35, no. 3, pp. 903–916, 1999.

[4] G. V. Trunk and S. F. George, "Detection of targets in non-gaussian sea clutter," *IEEE Transactions on Aerospace and Electronic Systems*, vol. AES-6, no. 5, pp. 620–628, 1970.

[5] D. C. Schleher, "Radar detection in weibull clutter," *IEEE Transactions on Aerospace and Electronic Systems*, vol. AES-12, no. 6, pp. 736–743, 1976.

[6] E. Jakeman and P. Pusey, "A model for non-rayleigh sea echo," *IEEE Transactions on Antennas and Propagation*, vol. 24, no. 6, pp. 806–814, 1976.

[7] K. Ward, "Compound representation of high resolution sea clutter," *Electronics letters*, vol. 16, no. 17, pp. 561–563, 1981.

[8] E. Conte and A. De Maio, "Mitigation techniques for non-gaussian sea clutter," *IEEE Journal of Oceanic Engineering*, vol. 29, no. 2, pp. 284–302, 2004.

[9] J. Xue, H. Li, M. Pan, and J. Liu, "Adaptive persymmetric detection for radar targets in correlated cg-ln sea clutter," *IEEE Transactions on Geoscience and Remote Sensing*, vol. 61, pp. 1–12, 2023.

[10] J. Xue, J. Liu, S. Xu, and M. Pan, "Adaptive detection of radar targets in heavy-tailed sea clutter with lognormal texture," *IEEE Transactions on Geoscience and Remote Sensing*, vol. 60, pp. 1–11, 2022.

[11] A. Balleri, A. Nehorai, and J. Wang, "Maximum likelihood estimation for compound-gaussian clutter with inverse gamma texture," *IEEE Transactions on Aerospace and Electronic Systems*, vol. 43, no. 2, pp. 775–779, 2007.

[12] Z. Wang, Z. He, Q. He, and Z. Cheng, "Persymmetric range-spread targets detection in compound gaussian sea clutter with inverse gaussian texture," *IEEE Geoscience and Remote Sensing Letters*, vol. 19, pp. 1–5, 2022.

[13] Q. Fuyong, M. Xiangwei, and L. Jianeng, "Adaptive censoring maximum likelihood cfar detector in weibull clutter," in *2011 Aerospace Conference*, 2011, pp. 1–7.

[14] L. P. Jiménez Jiménez, F. D. A. García, M. C. L. Alvarado, G. Fraidenraich, and E. R. d. Lima, "A general ca-cfar performance analysis for weibull-distributed clutter environments," *IEEE Geoscience and Remote Sensing Letters*, vol. 19, pp. 1–5, 2022.

[15] X. Zhang, R. Zhang, W. Sheng, X. Ma, Y. Han, J. Cui, and F. Kong, "Intelligent cfar detector for non-homogeneous weibull clutter environment based on skewness," in *2018 IEEE Radar Conference (RadarConf18)*, 2018, pp. 0322–0326.

[16] W. Zhou, J. Xie, B. Zhang, and G. Li, "Maximum likelihood detector in gamma-distributed sea clutter," *IEEE Geoscience and Remote Sensing Letters*, vol. 15, no. 11, pp. 1705–1709, 2018.

[17] D. S. Medeiros, F. D. A. García, R. Machado, J. C. S. S. Filho, and O. Saotome, "Ca-cfar performance in k-distributed sea clutter with fully correlated texture," *IEEE Geoscience and Remote Sensing Letters*, vol. 20, pp. 1–5, 2023.

[18] P. Huang, Z. Zou, X.-G. Xia, X. Liu, and G. Liao, "A statistical model based on modified generalized-k distribution for sea clutter," *IEEE Geoscience and Remote Sensing Letters*, vol. 19, pp. 1–5, 2022.

[19] H. M. Finn, "A cfar design for a window spanning two clutter fields," *IEEE Transactions on Aerospace and Electronic Systems*, vol. AES-22, no. 2, pp. 155–169, 1986.

[20] U. C. Doyuran and Y. Tanik, "Detection in range-heterogeneous weibull clutter," in *2007 IEEE Radar Conference*, 2007, pp. 343–347.

[21] S. Peng, L. Kong, and X. Yang, "A cfar algorithm for the non-homogeneous clutter background," in *Proceedings of 2011 IEEE CIE International Conference on Radar*, vol. 2, 2011, pp. 1721–1724.

[22] D. L. McCann and P. S. Bell, "A simple offset "calibration" method for the accurate geographic registration of ship-borne x-band radar intensity imagery," *IEEE Access*, vol. 6, pp. 13 939–13 948, 2018.

[23] ——, "Marine radar derived current vector mapping at a planned commercial tidal stream turbine array in the pentland firth, uk," in *2014 Oceans-St. John's*. IEEE, 2014, pp. 1–4.

[24] Hensoldt mk11 sharpeye. Last accessed 22-07-2024. [Online]. Available: ⟨https://uk.hensoldt.net/naval/kelvin-hughes-mk11-sharpeye/⟩

[25] W. S. Rosenberg, Luke, *Radar Sea Clutter - Modelling and Target Detection*. Institution of Engineering and Technology (The IET), 2022. [Online]. Available: https://app.knovel.com/hotlink/toc/id:kpRSCMTD01/radar-sea-clutter-modelling/radar-sea-clutter-modelling

[26] M. A. Richards *et al.*, *Fundamentals of radar signal processing*. Mcgraw-hill New York, 2005, vol. 1.

[27] W. M. Steki, "Sums of exponential random variables," Ph.D. dissertation, University of Nairobi, 2019.

[28] W. Magnus, F. Oberhettinger, R. P. Soni, and E. P. Wigner, "Formulas and theorems for the special functions of mathematical physics," *Physics Today*, vol. 20, no. 12, pp. 81–83, 1967.

DSPACE

https://dspace.org/

CFAR detection in heterogeneous K-distributed sea-clutter background

Mungara, Nagarakshith R.; Balleri, Alessio; Kocjancic, Leon; Acland, Tim

2024-10-21
Institute of Electrical and Electronics Engineers (IEEE)
https://doi.org/10.1109/radar58436.2024.10993546
Mungara N, Balleri A, Kocjancic L, Acland T. (2024) CFAR detection in heterogeneous K-distributed sea-clutter background. In: 2024 International Radar Conference (RADAR), 21-25 October 2024, Rennes, France

Downloaded from a DSpace repository. https://dspace.org/